Pramana – J. Phys. (2021) 95:74
https://doi.org/10.1007/s12043-021-02097-x

Energy transport analysis in the flow of Burgers nanofluid inspired by variable thermal conductivity

MASOOD KHAN, ZAHOOR IQBAL* and AWAIS AHMED

Department of Mathematics, Quaid-i-Azam University, Islamabad 44000, Pakistan
*Corresponding author. E-mail: izahoor@math.qau.edu.pk

MS received 5 April 2020; revised 7 December 2020; accepted 21 December 2020

Abstract. The rheology of Burgers nanofluid flow over a stretching cylinder with convective transport of thermal and solutal energy is studied in the present article. The relaxation and retardation properties of viscoelastic fluid are examined for flow field and energy distribution. Moreover, the thermophoretic and Brownian forces are also incorporated in the phenomena of thermal and solutal energy distribution. The thermal conductivity of the fluid is taken as temperature dependent. The homotopy analysis method (HAM) is adopted to solve the governing ordinary differential equations (ODEs). The impact of physical parameters on the flow field and energy transport is depicted using graphs. The outcomes proved that both thermophoretic and Brownian forces significantly boosted the temperature field but in the case of concentration field these show conflicting behaviour. The Burgers parameter of viscoelastic fluid enhances the thermal and solutal conduction in the fluid and decreases the fluid velocity. Moreover, due to the increase in temperature-dependent thermal conductivity, the transport of energy increases. The outcomes of this study are validated by comparing numerical data with some previous studies.

Keywords. Burgers nanofluid; variable thermal conductivity; heat transfer; heat generation/absorption; stretching cylinder.

PACS Nos **83.50.-v; 87.19.rh; 87.53.Vb; 83.60.Df**

1. Introduction

Non-Newtonian fluids are divided into three sub-categories, i.e, differential-type, integral-type and rate-type fluids. Physically, differential-type fluid models have shear thinning and thicking properties. Integral-type models correspond to memory fluids which means that they store the applied stress. Rate-type fluid models have the properties of fluid relaxation and retardation time phenomena. A Burgers fluid is basically a highly viscoelastic fluid with the phenomena of stress relaxation and creeping. As researchers and engineers pay attention to the topic of flow of viscoelastic material under certain circumstances, non-Newtonian viscoelastic materials have major roles in many physical applications. These materials are mainly employed in geophysical, biochemical and petrochemical industries. Scientists have done a lot of work on differential- and rate-type fluid models. Burgers fluid model is a widely established viscoelastic rate form fluid model. Burgers model has the ability to explain the stress relaxation and retardation in polymeric fluids. Initially, Maxwell (1866) developed the fluid model for the viscoelasticity of polymeric liquids to describe the stress relaxation phenomenon. Moreover, in his model demonstration at this time, he did not understand the mechanical point of view of the adoption of the spring and dashpot, but his research was in the direction of the energy storage and dissipation method. In contrast to this, the empirical model for studying material viscoelasticity in terms of relaxation and retardation times was introduced by Burgers [1]. This model is successfully applied to study the rheological characteristics of viscoelastic-type fluid, namely asphalt (see refs [2–6]). The boundary layer stagnation-point flow of Burgers liquid under the influence of Newtonian heating was explored by Hayat *et al* [7]. This effort revealed that the conjugate parameter enhances the temperature field near the surface. The Burgers fluid model was investigated by Waqas *et al* [8] by employing variable thermal conductivity and improved heat flux model. The properties of the nanofluid in the presence of chemical reaction and Lorentz force were examined

Published online: 03 May 2021

by Khan *et al* [9]. In recent investigations, Muhammad *et al* [10] studied the flow of Burgers nanofluid in porous medium immersed between two parallel plates by utilising heat rise/fall and thermal radiation effects. Elmaboud [11] investigated the free convective electro-osmotic flow of Burgers fluid through a vertical channel with Caputo–Fabrizio time-fractional derivative. It was found that due to electric double layer (EDL), the fluid flow velocity near the walls is higher, while in the core region, the opposite is noted. Some other recent studies on viscoelastic Burgers fluid can be found in refs [12–14].

The stretched cylinder-induced flow of viscous fluid has beneficial applications in industrial manufacturing and engineering. The fluid flow due to stretching cylinder was earlier examined by Crane [15]. Afterward, the time-independent flow of viscous fluid outside the walls of the cylinder was examined by Wang [16]. Moreover, Wang and Ng [17] also analysed the slip flow due to stretchable cylinder. Their results revealed that the velocity profile and shear stress at the surface decrease with higher slip parameter. Ashorynejad *et al* [18] assessed characteristics of nanofluid flow accelerated by a stretching geometry under the impact of Lorentz force. In addition, by taking into account the effects of nanoparticles and thermal radiation, Sheikholeslami *et al* [19] studied the thermal transport in the flow of fluid caused by permeable stretching cylinders. They found that concentration and thermal distribution are improved by amplifying the scales of curvature parameter. Flow of Casson fluid due to stretching cylinder was studied by Tamoor *et al* [20]. The analysis of thermal and solutal energy transport in the flow of non-Newtonian fluid was widely performed due to its importance in almost all engineering applications such as extrusion of polymer products, plastic coating etc. Hashim *et al* [21] assessed the thermal and solutal transport phenomena in Williamson fluid flow generated by a stretching cylinder under the influence of variable thermal conductivity effects. Asghar *et al* [22] reported the heat conduction features in the flow of Sisko fluid over a curved channel. The effects of variable viscosity and homogeneous–heterogeneous reactions on energy transport in the flow of Oldroyd-B fluid with Cattaneo–Christov theory were studied by Irfan *et al* [23]. This study proved that there is higher rate of thermal energy transport for large conductivity parameter. Khan *et al* [24] analysed the non-Fourier's heat flux model for heat transport in the transient flow of Maxwell fluid due to the stretching cylinder. The characteristics of thermophoretic and Brownian forces were studied in swirling flow of the Maxwell fluid with thermal and solutal energy transfer by Ahmed *et al* [25]. Some other recent investigations on heat transfer due to stretching geometries can be found in refs [26–28].

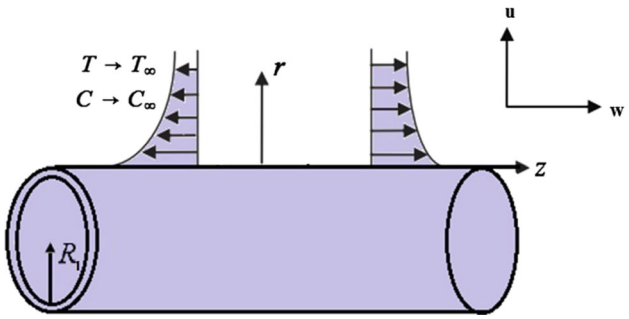

Figure 1. Flow configuration and coordinate system.

The present study is proposed in view of the aforementioned literature survey of non-Newtonian fluid flows due to stretching boundaries with heat and mass transport. The flow of viscoelastic Burgers nanofluid with thermal and solutal energy transport is considered here. The flow is produced due to stretching cylinder and the heat transfer in the flow is observed by employing variable thermal conductivity and heat source/sink effects. The developed model for the flow and energy transport is solved by employing homotopy analysis method (HAM). The comparison table is given which ensures the validation of homotopic approach.

2. Mathematical modelling

The 2D Burgers fluid flow is generated by the stretching boundary of the cylinder with radius R. The flow is further considered as time-independent and incompressible. The cylindrical polar coordinates (r, θ, z) are taken into account to model the flow and energy transport phenomena. The radial direction of the cylinder is taken along the r-axis while, the axis of the cylinder corresponds to z-axis as depicted in figure 1. Moreover, the corresponding velocities along r- and z-axes are taken as u and w. Hence, the velocity field for the current problem takes the form as $\mathbf{V} = [u, 0, w]$. In addition, it is realised that the stretching of the cylinder is produced along the z direction with velocity $w_s = U_0 z/l$, where l is the specific length and U_0 is the reference velocity. Moreover, (T_w, C_w) are considered as the temperature and concentration at the cylinder's surface, respectively.

Equations of continuity, momentum, heat and concentration for the current problem are as follows [13,14]:

$$\frac{\partial u}{\partial r}+\frac{u}{r}+\frac{\partial w}{\partial z}=0, \tag{1}$$

$$\begin{aligned}
&u\frac{\partial w}{\partial r}+w\frac{\partial w}{\partial z}+\lambda_1\left[u^2\frac{\partial^2 w}{\partial r^2}+w^2\frac{\partial^2 w}{\partial z^2}+2uw\frac{\partial^2 w}{\partial z\partial r}\right]\\
&\quad+\lambda_2\left[\begin{array}{l}
u^3\frac{\partial^3 w}{\partial r^3}+w^3\frac{\partial^3 w}{\partial z^3}+2u^2\left(\frac{\partial u}{\partial r}\frac{\partial^2 w}{\partial r^2}\right.\\
\left.+\frac{\partial w}{\partial r}\frac{\partial^2 w}{\partial r\partial z}\right)-u^2\left(\frac{\partial w}{\partial r}\frac{\partial^2 u}{\partial r^2}+\frac{\partial w}{\partial z}\frac{\partial^2 w}{\partial r^2}\right)\\
+2w^2\frac{\partial u}{\partial z}\frac{\partial^2 w}{\partial r\partial z}+w^2\left(\frac{\partial w}{\partial z}\frac{\partial^2 w}{\partial z^2}\right.\\
\left.-\frac{\partial w}{\partial r}\frac{\partial^2 u}{\partial z^2}\right)+3uw\left(u\frac{\partial^3 w}{\partial r^2\partial z}+w\frac{\partial^3 w}{\partial z^2\partial r}\right)\\
+2uw\left(\frac{\partial u}{\partial r}\frac{\partial^2 w}{\partial z\partial r}+\frac{\partial u}{\partial z}\frac{\partial^2 w}{\partial r^2}\right.\\
\left.+\frac{\partial w}{\partial r}\frac{\partial^2 w}{\partial z^2}-\frac{\partial w}{\partial r}\frac{\partial^2 u}{\partial r\partial z}\right)
\end{array}\right]\\
&=\nu\lambda_3\left[\begin{array}{l}
u\frac{\partial^3 w}{\partial r^3}+w\frac{\partial^3 w}{\partial r^2\partial z}+\frac{u}{r}\frac{\partial^2 w}{\partial r^2}-\frac{\partial w}{\partial r}\frac{\partial^2 u}{\partial r^2}\\
+\frac{w}{r}\frac{\partial^2 w}{\partial r\partial z}-\frac{1}{r}\frac{\partial u}{\partial r}\frac{\partial w}{\partial r}\\
-\frac{1}{r}\frac{\partial w}{\partial r}\frac{\partial w}{\partial z}-\frac{\partial w}{\partial z}\frac{\partial^2 w}{\partial r^2}
\end{array}\right]\\
&\quad+\nu\left[\frac{\partial^2 w}{\partial r^2}+\frac{1}{r}\frac{\partial w}{\partial r}\right],
\end{aligned} \tag{2}$$

$$\begin{aligned}
&u\frac{\partial T}{\partial r}+w\frac{\partial T}{\partial z}=\frac{1}{(\rho c_p)}\frac{1}{r}\left[\frac{\partial}{\partial r}\left(K(T)\frac{\partial T}{\partial r}\right)\right]\\
&\quad+\tau\left[D_b\frac{\partial C}{\partial r}\frac{\partial T}{\partial r}+\frac{D_T}{T_\infty}\left(\frac{\partial T}{\partial r}\right)^2\right]\\
&\quad+\frac{Q_0(T-T_\infty)}{\rho c_p},
\end{aligned} \tag{3}$$

$$\begin{aligned}
&u\frac{\partial C}{\partial r}+w\frac{\partial C}{\partial z}=\frac{D_B}{r}\frac{\partial}{\partial r}\left(r\frac{\partial C}{\partial r}\right)\\
&\quad+\frac{D_T}{T_\infty}\frac{1}{r}\frac{\partial}{\partial r}\left(r\frac{\partial T}{\partial r}\right),
\end{aligned} \tag{4}$$

with boundary conditions

$$w=\frac{U_0 z}{l},\ u=0,\ T=T_w,\ C=C_w \quad \text{at } r=R, \tag{5}$$

$$w\to 0,\ \frac{\partial w}{\partial r}\to 0,\ T\to T_\infty,\ C\to C_\infty \text{ as } r\to\infty. \tag{6}$$

Here λ_1 is the fluid relaxation time, λ_2 is the material parameter of Burgers fluid, λ_3 is the fluid retardation time, (T, C) are the liquid temperature and concentration respectively, (T_∞, C_∞) are the ambient temperature and concentration respectively, ρ is the density of the liquid, Q_0 is the heat generation/absorption coefficient, τ is the heat capacity ratio, D_B is the mass diffusivity, D_T is the thermophoresis coefficient, c_p is the specific heat, ν is the kinematics viscosity, p is the pressure and $K(T)$ is the variable thermal conductivity of the liquid which is explained by the following relation:

$$K(T)=k_\infty\left[1+\epsilon\left(\frac{T-T_\infty}{T_w-T_0}\right)\right],$$

where k_∞ is the thermal conductivity of the nanofluid far away from the stretched surface while ϵ is the thermal conductivity parameter.

By employing the following conversions [12,20,21]

$$\begin{aligned}
&u=-\frac{R}{r}\sqrt{\frac{U_0\nu}{l}}f(\eta),\quad w=\frac{U_0 z}{l}f'(\eta),\\
&\theta(\eta)=\frac{T-T_\infty}{T_w-T_\infty},\\
&\phi(\eta)=\frac{C-C_\infty}{C_w-C_\infty},\\
&\eta=\sqrt{\frac{U_0}{\nu l}}\left(\frac{r^2-R^2}{2R}\right).
\end{aligned} \tag{7}$$

By employing overhead substitutions, eq. (1) is satisfied automatically and eqs (2)–(4) give the following forms [12,13]:

$$\begin{aligned}
&(1+2\alpha\eta)^2\beta_1\left[2ff'f''-f^2f'''\right]\\
&-4\alpha\beta_3(1+2\alpha\eta)^2 ff'''-4\alpha^2\beta_2 f'''f''\\
&+(1+2\alpha\eta)^3 f'''\\
&-(1+2\alpha\eta)^2\beta_2[3f^2(f'')^2+2f(f')^2f''-f^3f^{iv}]\\
&-(1+2\alpha\eta)\alpha\beta_1 f^2f''\\
&+(1+2\alpha\eta)\alpha\beta_2\left[3f^2f'f''+f^3f'''\right]\\
&+(1+2\alpha\eta)^2[2\alpha f''+ff''-(f')^2]\\
&+(1+2\alpha\eta)^3\beta_3[(f'')^2-ff^{iv}]=0.
\end{aligned} \tag{8}$$

$$\begin{aligned}
&(1+2\alpha\eta)\theta''+2\alpha\theta'+(1+2\alpha\eta)\\
&\times(\theta\theta''+\theta'^2)\epsilon+2\alpha\epsilon\theta\theta'+\mathrm{Pr}\, f\theta'+\mathrm{Pr}\,\delta\theta\\
&+\mathrm{Pr}\, N_b\phi'\theta'(1+2\alpha\eta)\\
&+\mathrm{Pr}\, N_t\theta'^2(1+2\alpha\eta)=0,
\end{aligned} \tag{9}$$

$$\begin{aligned}
&(1+2\alpha\eta)\phi''+2\alpha\phi'\\
&+\mathrm{Le}\,\mathrm{Pr}\, f\phi'+(1+2\alpha\eta)\left(\frac{N_t}{N_b}\right)\theta''\\
&+2\alpha\left(\frac{N_t}{N_b}\right)\theta'=0,
\end{aligned} \tag{10}$$

and the transformed boundary conditions are as follows:

$$f=0,\ f'=1,\ \theta=1,\ \phi=1 \quad \text{at } \eta=0, \tag{11}$$

$$f'\to 0,\ f''\to 0,\ \theta\to 0,\ \phi\to 0 \quad \text{as } \eta\to\infty, \tag{12}$$

where Deborah numbers β_1 and β_3, the curvature parameter α, Burgers fluid parameter β_2, Prandtl number Pr,

heat rise/fall parameter δ, thermophoresis parameter N_t, Lewis number Le and Brownian motion parameter N_b are defined as follows:

$$\beta_1 = \lambda_1 \frac{U_0}{l}, \quad \beta_2 = \lambda_2 \left(\frac{U_0}{l}\right)^2,$$
$$\beta_3 = \lambda_3 \frac{U_0}{l}, \quad \alpha = \frac{1}{R}\sqrt{\frac{\nu l}{U_0}},$$
$$\delta = \frac{l Q_0}{U_0 (\rho c)_f},$$
$$\Pr = \frac{\nu}{\alpha_1}, \quad N_t = \frac{\tau D_T (T_w - T_\infty)}{\nu T_\infty},$$
$$Le = \frac{\alpha_1}{D_B}, \quad N_b = \frac{\tau D_B (C_w - C_\infty)}{\nu}. \tag{13}$$

3. Homotopic approach

This section is adopted to employ HAM for finding the series solution of the problem under consideration. We require initial guesses and linear operators to start with HAM. For this purpose, we have chosen (f_0, θ_0, ϕ_0) as initial guesses and $(\pounds_f, \pounds_\theta, \pounds_\phi)$ as the corresponding linear operators. Some previously published studies also employed HAM to solve the ODEs [8,9,13].

$$f_0(\eta) = 1 - \mathrm{e}^{-\eta}, \quad \theta_0(\eta) = \mathrm{e}^{-\eta},$$
$$\phi_0(\eta) = \mathrm{e}^{-\eta} \tag{14}$$
$$\pounds_f[f(\eta) = f''' - f', \quad \pounds_\theta[\theta(\eta)] = \theta'' - \theta,$$
$$\pounds_\phi[\phi(\eta)] = \phi'' - \phi. \tag{15}$$

4. Physical analysis of the outcomes

As the adopted ordinary differential equations (8)–(11) are coupled and nonlinear of fourth order, it is difficult to tackle these equations analytically and hence we employed HAM to find semi-analytic solutions of differential equations (8)–(11) with boundary conditions (12) and (13). By employing this homotopic technique we assessed the effects of pertinent physical parameters on velocity $f'(\eta)$, thermal $\theta(\eta)$ and solutal $\phi(\eta)$ distributions of Burgers fluid. We allocated fixed magnitudes for leading constraints such as $\alpha = 0.8$, $\beta_1 = 0.55$, $\beta_2 = 0.17$, $\beta_3 = 0.3$, $\Pr = 7.0$, Le$= 7.5$, $N_b = 0.7$, $N_t = 0.9$, $\delta = 1.5$, $\epsilon = 0.9$ during the entire computations. We explored the physical intimation of relaxation time parameter β_1, Burgers fluid parameter β_2, curvature parameter α on flow, thermal and solutal profiles. Moreover, the effects of thermophoretic force parameter N_t, Brownian motion parameter N_b, heat source/sink parameter δ, variable thermal conductivity parameter ϵ, Prandtl number Pr and Lewis number Le on thermal and concentration profiles are also checked. The behaviour of all physical constraints are depicted physically in figures 2–9.

The behaviour of all physical parameters is justified by reasonable arguments. The effect of fluid relaxation time parameter (β_1) on velocity, thermal and solutal distributions is shown in figures 2a– 2c. These figures illustrate that the increasing values of β_1 de-accelerate the flow velocity and the corresponding boundary layer thickness of Burgers fluid. In contrast, a significant growth is noted in the transport of thermal and solutal energy for incrementing scales of β_1. Actually, due to increment in relaxation time paramaters the resistance among the fluid particles enhances, thus flow field declines while the transport of thermal and solutal energy in the flow rises. To highlight the features of velocity profile, thermal distribution and nanoparticles volume fraction profile for increasing values of Burgers fluid parameter (β_2), figures 3a–3c are plotted. From these plots, one can assess that the increase in β_2 decreases the velocity of the fluid while the heat conduction and mass diffusion process increase for increased values of β_2. The velocity and thermal boundary conditions are asymptotically satisfied in the region. Thickness of thermal boundary layer also seems to increase for augmented values of β_2. The effect of curvature parameter (α) on momentum transport, heat conduction and mass diffusion phenomena are displayed in figures 4a–4c. It can be seen that, higher values of α accelerates the momentum transport as well as the thermal and solutal transport in the flow of Burgers nanofluid. Moreover, the velocity and thermal boundary layer thickness increase for increasing values of α. Physically, the enlargement of the curvature results in the deterioration of the radius of the cylinder which implies the reduction in the interface of the fluid and cylinder surface region. Therefore, the resistance on the fluid due to exterior becomes less leading to the acceleration of the flow velocity in the region. Moreover, the larger heat transport corresponds to the increased thermal profile of Burgers fluid. Figures 5a and 5b depict the effect of thermophoretic force parameter (N_t) on the profiles of thermal and solutal transport. One can easily detect that increasing values of N_t promote the thermal as well as the solutal transport in the flow. Hence, the thermal and concentration curves of Burgers fluid increases for higher trend in N_t. Basically, during thermophoresis the fluid particles move from hotter to colder zones which serves to boost the kinetic energy of the system and hence there will be a build-up of thermal and concentration profiles. The features of thermal profile and concentration

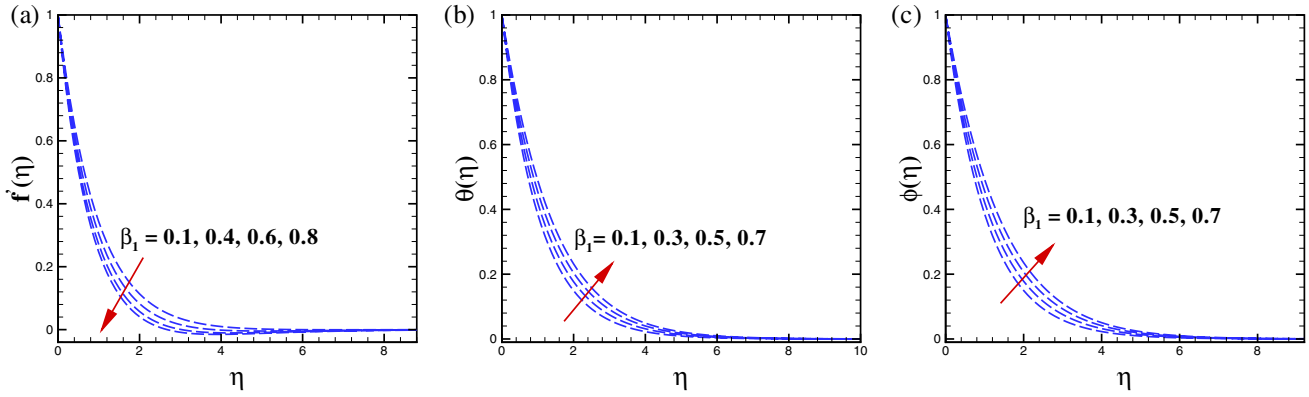

Figure 2. (**a**)–(**c**) Impact of β_1 on f', θ and ϕ.

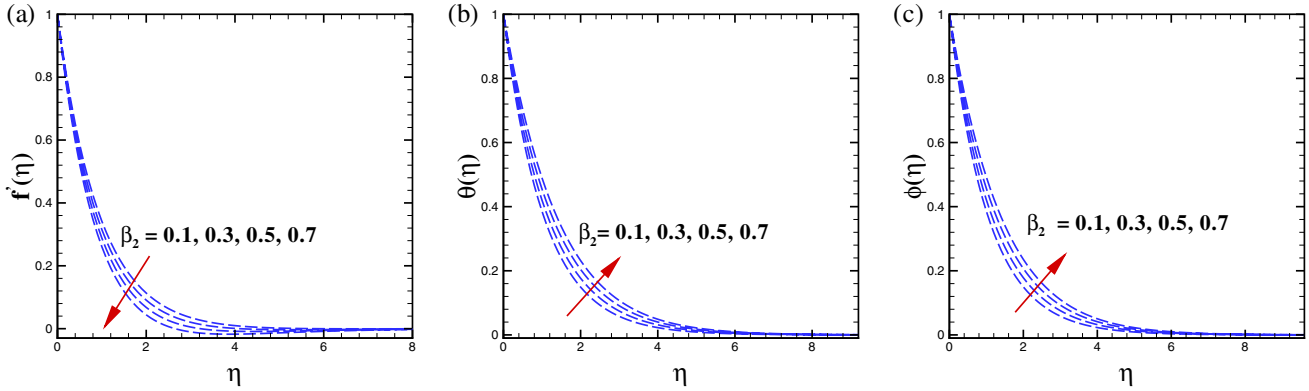

Figure 3. (**a**)–(**c**) Effect of β_2 on f', θ and ϕ.

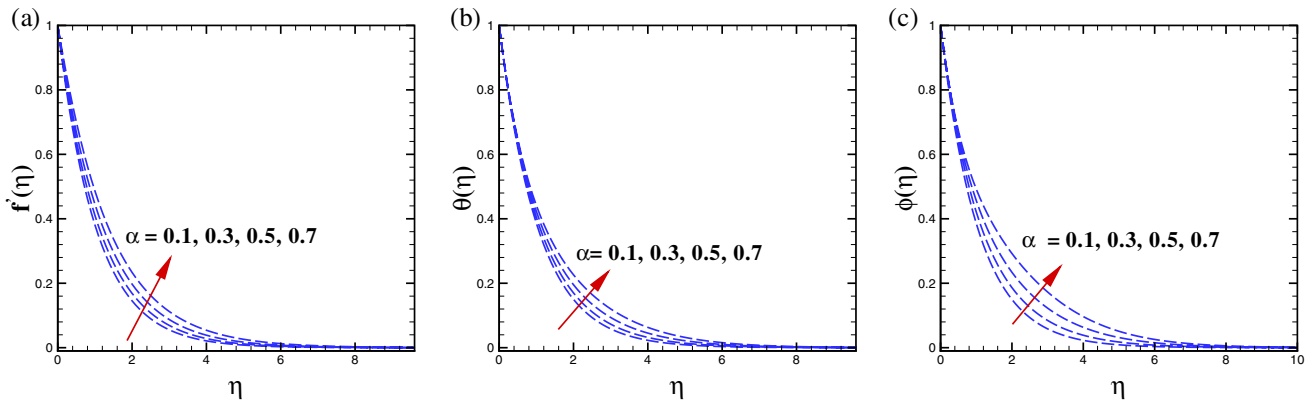

Figure 4. (**a**)–(**c**) Effect of α on f', θ and ϕ.

distribution in response of Brownian motion constraint (N_b) are illustrated graphically in figures 6a and 6b. It can be seen that, the higher value of N_b promotes the heat transform phenomenon in the flow while, the mass diffusion process decreases for incrementing N_b. The thermal thickness of the boundary layer significantly improves for the building blocks of N_b and the thermal boundary conditions are satisfied asymptotically throughout the solution region. In Brownian motion, the random movement of particles increases the collision among fluid elements due to which kinetic energy of the system increases which corresponds to the intensified thermal distribution of the nanofluid. On the other hand, the diminishing trend of mass transport is the consequence of the fact that the mass transfer phenomenon is disturbed due to the collision of fluid particles for incrementing N_b. The effects of Pr and Le on temperature and concentration fields are

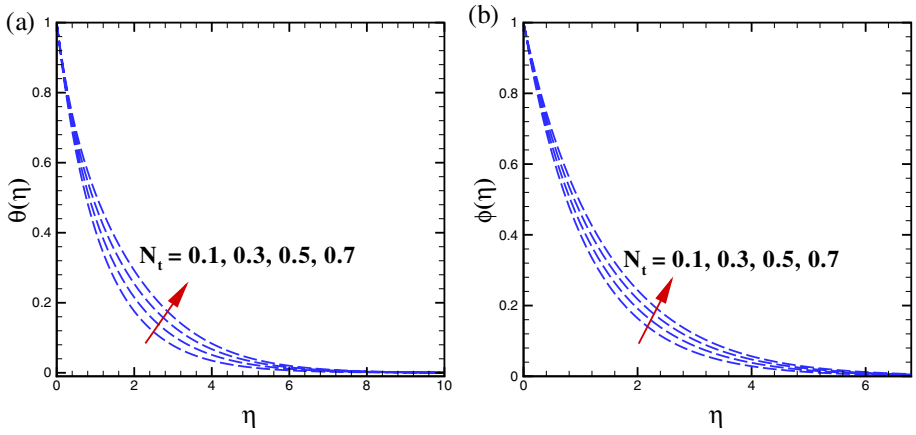

Figure 5. Effect of N_t on θ and ϕ.

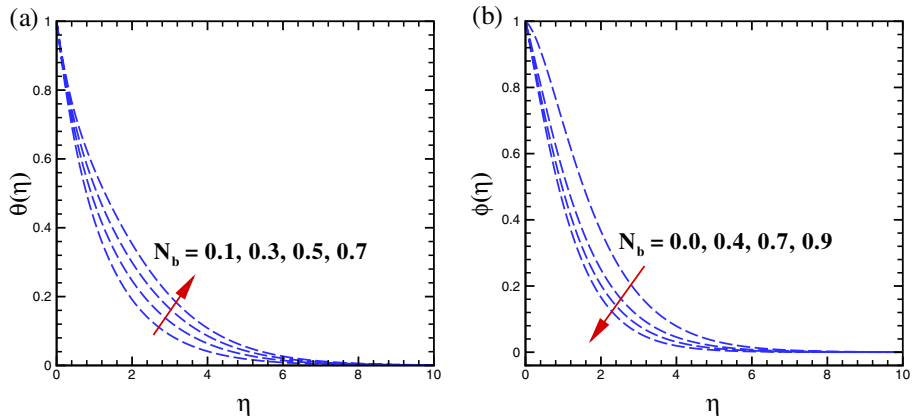

Figure 6. (**a**), (**b**) Effect of N_b on θ and ϕ.

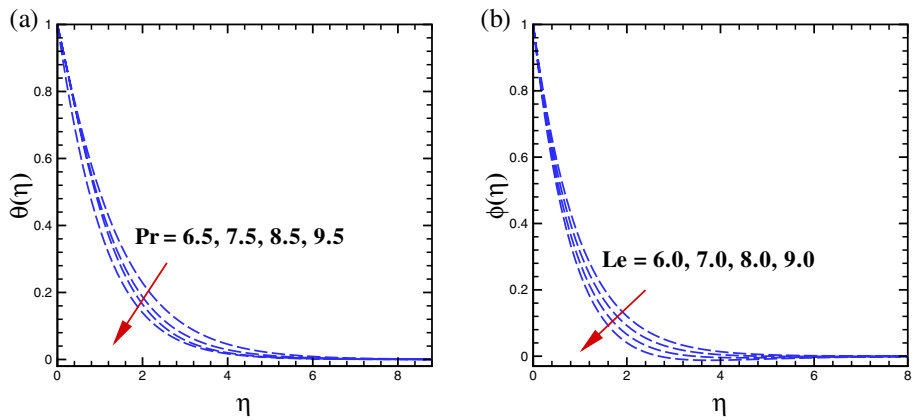

Figure 7. (**a**), (**b**) Effect of Pr and Le on temperature and concentration field.

shown in figures 7a and 7b. The depreciating trend of thermal and solutal distributions is being presumed for higher values of Pr and Le, respectively. It is because of the fact that, mathematically the Prandtl number is in inverse relation with thermal diffusion coefficient and an escalation in the Pr corresponds to lower thermal diffusivity.Obviously, lesser thermal diffusivity decreases the heat transport in the Burgers fluid flow. Similarly, increased Le results in lower mass diffusivity which decreases the nanoparticle volume fraction profile. Figure 8 is drawn to show the impact of temperature-dependent thermal conductivity

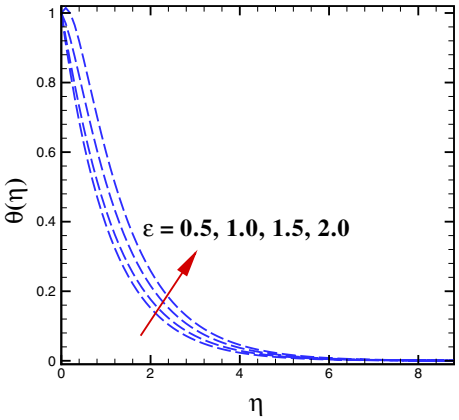

Figure 8. Impact of ϵ on temperature profile.

Table 1. A comparison table for $-f''(0)$ against different values of β_1 when $\alpha = \beta_2 = \beta_3 = \text{Pr} = \text{Le} = \delta = N_b = N_t = \epsilon = 0$.

β_1	Abel *et al* [29]	Waqas *et al* [30]	Present study
0.0	1.000000	1.000000	1.0000000
0.2	1.051948	1.051889	1.0518889
0.4	1.101850	1.101903	1.1019041
0.6	1.150163	1.150137	1.1501369
0.8	1.196692	1.196711	1.1967045
1.0	–	–	1.2417689
1.2	1.285257	1.285363	1.2853712
1.4	–	–	1.3276671
1.6	10368641	1.368758	1.3687581
1.8	–	–	1.4087309
2.0	1.447617	1.447651	1.4476509

constraint (ϵ) on thermal transport of Burgers fluid. This figure shows that, the larger ϵ accelerates the transport of heat energy in the flow. This is the consequence of the enhanced thermal conductivity of the fluid. The larger thermal conductivity serves to transform more heat to the fluid from the surface of the cylinder which results in the intensification of the thermal profile of the Burgers fluid. Figures 9a and 9b are shown to describe the consequence of heat rise ($\delta > 0$) and heat fall ($\delta < 0$) constraints on heat transfer phenomenon in Burgers nanofluid. Clearly, the thermal transport in the flow seems to be accelerated by the escalation in the magnitude of heat rise parameter while the thermal transport declines for the building amount of heat fall parameter. Physically, the building up of thermal profile is the consequence of the intensification in the heat source because more heat stores in the system which promotes the thermal transport whereas, the situation is opposite in the heat sink case. In case of heat sink in the system, the thermal energy loses from the system and thus, the temperature profile declines. Table 1 is a comparison table of $-f''(0)$ for several values of β_1 which shows that the current study is in best agreement with some previously published studies in reducing case.

5. Concluding remarks

The features of relaxation and creeping phenomena of viscoelastic Burgers nanofluid flow induced above the stretching cylinder are studied. The thermal and solutal analyses are also carried out in view of thermophoretic and Brownian forces. The conductivity of the fluid is assumed as variable with uniform source/sink for heat. The study is concluded in the following way:

- The thermophoretic force in the fluid enhances the convective heat and mass transport.

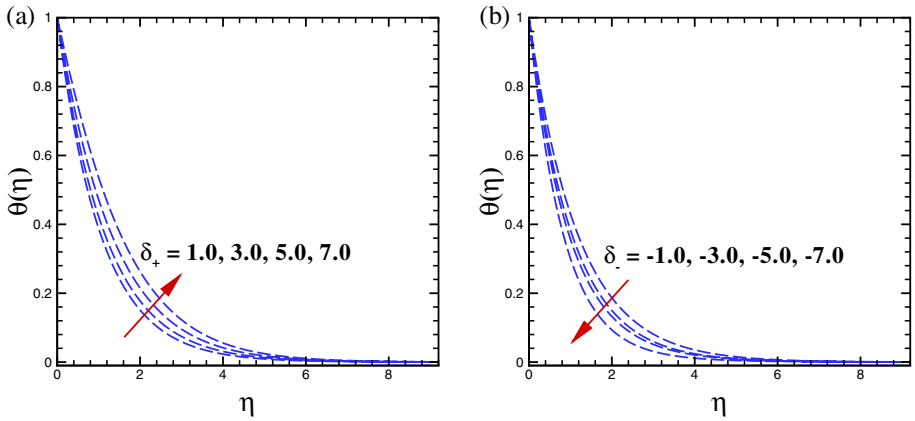

Figure 9. (**a**), (**b**) Effect of heat generation ($\delta > 0$) and absorption ($\delta < 0$) on temperature profiles.

- The developing phenomenon of relaxation time decreases the flow field but increases the energy transport.
- Temperature field increases in the case of escalating small conductivity parameter.
- Thermal and solutal profiles increase in the case of high creeping mechanism. Inverse trend is noted for the flow field.
- Thermal diffusivity of the nanofluid decreases when Prandtl number increases.
- An increase in curvature parameter increases the flow velocity and energy transport phenomenon.
- The thermal transport in the flow is accelerated for increasing values of heat source constraint while it diminishes for heat sink constraint.

References

[1] J M Burgers, *Mechanical considerations – Model systems – phenomenological theories of relaxation and of Viscosity* (1939)

[2] A R Lee and A H D Markwick, *J. Soc. Chem. Indust*. **56**, 146 (1937)

[3] R N J Saal and J W A Labout, Rheological properties of asphalts, in: *Rheology: Theory and applications* edited by F R Eirich (Academic Press, New York,1958) Vol. 2, pp. 363–400

[4] C L Monismith and K E Secor, *Viscoelastic behavior of asphalt concrete pavements* (Inst. of Transportation and Traffic Eng., Univ. of California, Berkeley, 1962)

[5] C L Monismith, R L Alexander and K E Secor, *Proc. Assoc. Asph. Paving Technol. Tech. Sess*. **35**, 400 (1966)

[6] J M Muralikrishnan and K R Rajagopal, *Appl. Mech. Rev*. **56**, 149 (2003)

[7] T Hayat, S Ali, M Awais and M S Alhuthali, *Appl. Math. Mech.* **36**(**1**), 61 (2015)

[8] M Waqas, T Hayat, M Farooq, S A Shehzad and A Alsaedi, *J. Mol. Liq*. **220**, 642 (2016)

[9] W A Khan, M Irfan, M Khan, A S Alshomrani, A K Alzahrani and M S Alghamdi, *J. Mol. Liq*. **234**, 201 (2017)

[10] S Muhammad, S I A Shah, G Ali, M Ishaq, S A Hussain and Z Shah, *J. Nanofluids* **8**(**5**), 957 (2019)

[11] Y Abd Elmaboud, *Alex. Eng. J.* (2020), https://doi.org/10.1016/j.aej.2020.08.012

[12] Z Iqbal, M Khan, A Ahmed and S Nadeem, *Phys. Scr*. (2020), https://doi.org/10.1088/1402-4896/abc381

[13] M Khan, Z Iqbal and A Ahmed, *J. Therm. Anal. Calorim.* (2020), https://doi.org/10.1007/s10973-020-10224

[14] Z Iqbal, M Khan and A Ahmed, *J. Therm. Anal. Calorim*. (2020), https://doi.org/10.1007/s10973-020-10308

[15] L J Crane, *Z. Angew. Math. Phys.* **26**, 619 (1975)

[16] C Y Wang, *Phys. Fluids* **31**, 466 (1988)

[17] C Y Wang and C O Ng, *Int. J. Non-Linear Mech.* **46**, 1191 (2011)

[18] H R Ashorynejad, M Sheikholeslami, I Pop and D D Ganji, *Heat Mass Transf*. **49**, 427 (2013)

[19] M Sheikholeslami, M T Mustafa and D D Ganji, *Iran. J. Sci. Technol.* **39**, 433 (2015)

[20] M Tamoor, M Waqas, M I Khan, A Alsaedi and T Hayat, *Results Phys*. **7**, 498 (2017)

[21] A Hashim, A Hamid and M Khan, *Microsystem Technologies* **25**, 3287 (2019)

[22] Z Asghar, N Ali, R Ahmed, M Waqas and W A Khan, *Comp. Meth. Prog. Biomedicine* **182**, 105040 (2019)

[23] M Irfan, M Khan and W A Khan, *J. Braz. Soc. Mech. Sci. Eng*. **41(3)**, 1 (2019)

[24] M Khan, A Ahmed, M Irfan and J Ahmed, *J. Therm. Anal. Calorim*. (2020), https://doi.org/10.1007/s10973-020-09343-1

[25] A Ahmed, M Khan and J Ahmed, *Appl. Math. Mech*. **41**, 1417 (2020)

[26] Z Iqbal, M Khan, A Ahmed, J Ahmed and A Hafeez, *Appl. Nanosci*. (2020), https://doi.org/10.1007/s13204-020-01386-y

[27] M Khan, Z Iqbal and A Ahmed, *Appl. Nanosci.* (2020), https://doi.org/10.1007/s13204-020-01360-8

[28] Z Iqbal, M Khan and A Ahmed, *Euro. Phys. J. Appl. Phys.* (2020), https://doi.org/10.1051/epjap/2020200286

[29] M S Abel, J V Tawade and M M Nandeppanavar, *Meccanica* **47**, 385 (2012)

[30] M Waqas, M I Khan, T Hayat and A Alsaedi, *Res. Phys*. **7**, 2489 (2017)